THE MOTION OF EXPLOSION PRODUCTS BEHIND THE FRONT OF A DETONATION WAVE

V. N. Zubarev

Zhurnal Prikladnoi Mekhaniki i Tekhnicheskoi Fiziki, No. 2, pp. 54-61, 1965

The velocity of the explosion products behind the detonation wavefront in a 50/50 TNT-hexogen explosive was measured by an electromagnetic method.

The experimental data on the mass velocity profile behind the wavefront in charges of different lengths, and the results of measurements of the motion of the backward rarefaction waves can be well described if in the mass velocity-time curves one isolates a stationary zone of ~0.1 μsec and regards the rest of the motion as self-similar.

The experimentally observed sharp drop of mass velocity behind the wavefront indicates that the isentropic exponent of the explosion products increases upon expansion.

The observed data on the distribution of mass velocities were used to calculate the isentrope of the explosion products in the pressure range 100-250 000 atm.

In the self-similar region of a detonation, the motion of the explosion products (EP) behind the detonation wavefront is uniquely determined by the parameters of their isentropic expansion curve.

For the case of power-law isentropes $p = A\rho^n$ (A and n constant), Ya. B. Zel'dovich [1] has derived linear relations between the mass velocity u and the speed of sound c and the dimensionless parameter $\xi = x/Dt$ (D is the detonation velocity). In this solution the values of u and c decrease linearly from their values at the Jouguet point, $u_j = D/(n + 1)$, $c_j = nD/(n + 1)$, to 0 and D/2 at $\xi = 1/2$.

A different result was obtained by Taylor [2], who solved the same problem for the particular case of the TNT isentrope [3]. The relation obtained in [2] differs markedly from a linear relation (it has negative curvature near the wavefront, with a point of inflection at $\xi \approx 0.85$).

The considerable discrepancy between the theoretical expressions for $u(\xi)$ for different EP isentropes indicates the possibility of solving the inverse problem: calculating the expansion isentrope of the EP from experimental data on their motion.

The present research, carried out in 1956-58, was aimed at solving this problem by measuring the mass-velocity distribution during the detonation of solid explosives.

One possible source of information on the variation of the mass velocity of an EP in a detonation wave is provided by measurements of the shock intensity in obstacles [4-8]. Such measurements have yielded the parameters of the Jouguet point and the width of the high pressure zone [7, 8]. These data have also made it possible to draw certain conclusions regarding the mass velocity distribution behind a detonation wavefront.

An analysis of the attenuation of shock waves in obstacles was carried out by Drummond [9], who related the rate of attenuation of the shock in the obstacle to the parameters of the isentrope of the EP and thus chose the isentropic relation that best agreed with the experimental data. The results are referred to states near the Jouguet point, which is typical for shock measurements in obstacles. The method makes it possible to measure only a narrow region of states adjacent to the detonation wavefront. The study of more distant regions by this method is quite difficult. Similar investigations can be carried out quite effectively by the electromagnetic method of measuring wave and mass velocities, proposed by E. K. Zavoiskii in 1948 and developed by V. A. Tsukerman and A. A. Brish*. This method makes it possible to obtain data on the motion of matter behind the fronts of shock and detonation waves, in particular in the study of states remote from the front.

Some of the results obtained by E. K. Zavoiskii and V. A. Tsukerman were reproduced and extended by V. M. Zaitsev [10]. In our research we used the electromagnetic method (EM) of recording the mass velocity distribution in the rarefaction wave behind a detonation shock.

Experimental set-up and measuring method. In the EM method of continuous recording of mass velocities, the

*These authors also determined the effect of the conductivity of the EP on the results of the measurements and developed the sensing devices, which were also used in the present research.

measured variable is the emf ($\varepsilon(\tau)$) induced by the motion of a conductor in a magnetic field H. For the experimental scheme* represented in Fig. 1 we have

$$\varepsilon(\tau) = lHu(\tau)10^{-8}\ \text{V}.$$

Here l, u, and H are measured in cm, cm/sec, and oersteds, respectively. Assuming that the cross-piece of the sensor is carried away by the explosion products, one can determine the velocity distribution behind the shock front from the relation $\varepsilon(\tau)$.

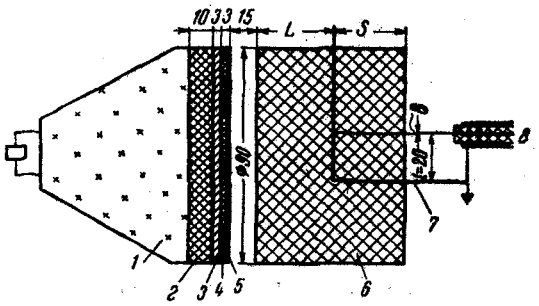

Fig. 1

The magnetic field of ~100 Oe, inside which the charge was detonated, was generated by electromagnets of ~200 × 200 mm cross section. Possible errors due to the inhomogeneity of the field along the path of the sensor and to the change of field intensity with time did not exceed 0.1%. The signal of ~1 V induced by the motion of the sensor was transmitted through cable 8 to a double-beam oscilloscope OK-17M with a wide-band amplifier. Inaccuracies due to the nonlinearity of the amplitude characteristic (~10%) were eliminated by the use of calibration curves.

A general check of the measuring method was carried out by measuring the mass velocity behind a shock wave in paraffin. The amplitude of the wave in paraffin was independently determined by the "splitting-off" method [5]. The values** obtained by the two methods practically coincided (2.03 ± 0.035 and 2.04 ± 0.04 km/sec), which confirms the validity of the values obtained by the EM method.

The experiments were carried out with charges of 50/50 TNT-hexogen. The quality of each casting and the positioning of the sensor in the charge were X-ray controlled. The detonation velocity was 7.65 km/sec and the density of the charge 1.68 g/cm^3.

In order to eliminate nonuniformities due to the effect of the sides, we restricted the length-to-diameter ratio of the charge to less than 2/3.

The II-form aluminum-foil sensor 7 (Fig. 1) was positioned in the course of casting the charge. The length and width of the cross-piece were ~20 mm each, and the legs were S ~ 30 mm. This length allowed ~4 μsec recording time before the detonation passed the end face of the charge.

Thickness of the sensor had to be made as small as possible, in order to avoid inertia effects. The experiments were carried out with foil of thickness δ = 0.1-0.2 mm. Further reduction in thickness led to errors associated with the natural conductivity of the explosion products.

According to [11], the conducting zone in a detonation wave is a thin layer near the front, whose resistance is of the order of 0.1 Ω. For this value and a sensor 0.1 mm thick, in the most unfavorable case the motion of the conducting layer of the EP in the magnetic field would lead to an increase in the velocity reading of ~20 m/sec, which is comparable with the random error (~50 m/sec). Thus, further reduction in sensor thickness is inadmissible.

The complex method of initiation, illustrated in Fig. 1, guaranteed instantaneous initiation of the charge over its surface. Initiation was carried out by means of a thin (0.05 mm) aluminum foil 5, accelerated in the air gap (15 mm) to a velocity of ~5 km/sec, which is sufficient to initiate the charge without a delay. In this case the time of application of high pressure was of the order of the time of passage of the shock wave through the foil, i.e., ~0.01 μsec, which is of the same order as the width of the high pressure zone in the detonation wave [7, 8].

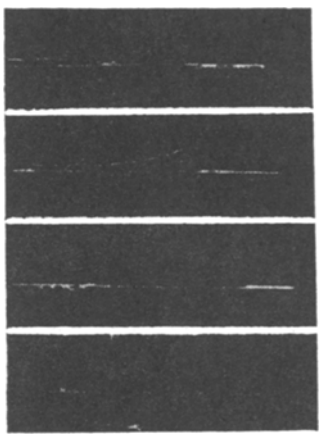
Fig. 2

The explosive layer 4, which accelerated the foil 5, was separated from the lens charge 1-2 by a lead spacer 3. This eliminated the effect of the EP of charge 1-2 on the detonation wave of charge 6.

The nonuniformities of the detonation wavefront obtained by this method did not exceed 1 mm.

Recording of mass velocities in charges of different lengths. Relations of the form $u(\tau)$ were determined experimentally for charges 5 to 60 mm in length. The time τ was measured from the arrival of the detonation wave at the sensor. On the oscillograms this moment was identified by a vertical deflection of the beam. Figure 2 shows the oscillo-

*The magnetic field is normal to the plane of the drawing.

**Means of ten experiments.

grams of the mass velocities. Reading from the top down, the frames correspond to charge lengths L = 5, 15, 30, and 60 mm, respectively (L is the length from the end face of the charge to the cross-piece of the sensor, Fig. 1). The upper beam records the mass velocity (the arrow shows the direction of scanning), and the lower beam shows the time scale (10 megacycle frequency). Figure 2 qualitatively confirms the theoretical result that the mass velocity decreases monotonically at a rate which increases with decreasing charge length.

A quantitative comparison of the curves $u(\tau)$ is given in Fig. 3, which represents the means of four-to-six experiments, corresponding to charge lengths: a) 5 mm, b) 15 mm, c) 30 mm, d) 60 mm. The abscissas of Fig. 3a represent $\tau = \tau_e$ (τ_e is the experimentally determined time). These relations can be used to check the self-similarity of the detonation wave directly.

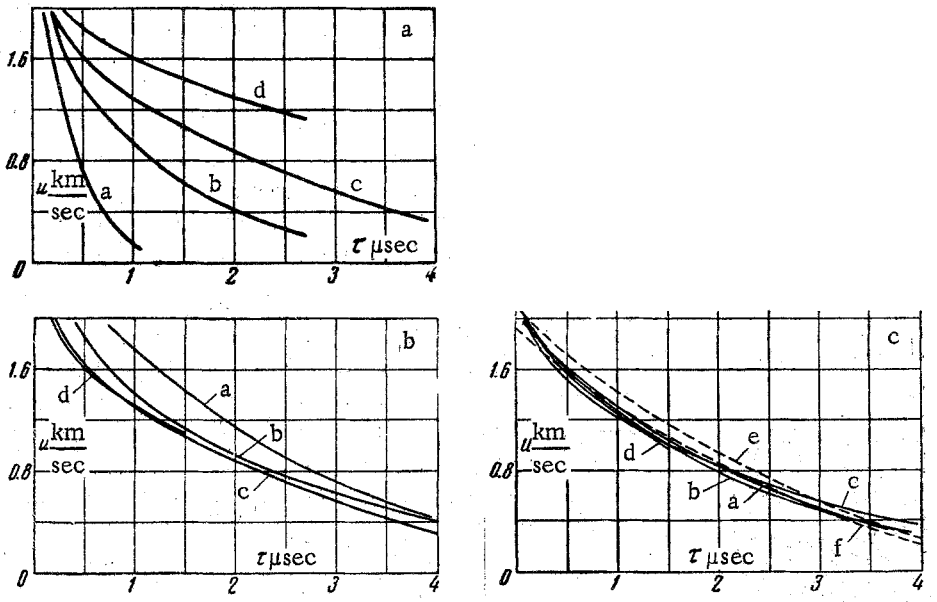

Fig. 3

If the wave is self-similar, then the change in the time scale should be proportional to the charge length. Consequently, all curves $u_i(\tau)$ redrawn in the coordinates u_i, $\tau_e L_0/L_i$ should coincide with Fig. 3a. The results of this construction are shown in Fig. 3b (L_0 = 30 mm). The large discrepancy between the curves in that figure indicates that the deviations from self-similarity are still large when the wave has traveled ~10 mm. But even for L > 30 mm the deviation from self-similarity is already negligible, as can be seen from the congruence of the curves for long charges (L = 30 and 60 mm, Fig. 3b).

Moreover, as can be seen in Fig. 3b, the curves $u_i(\tau_e L_0/L_i)$ are arranged in a definite sequence, those corresponding to shorter charge lengths L_i lying to the right. This indicates that it might be advisable to shift the time origin by some value τ_0, equal for all curves of Fig. 3a.

The results of shifting the time origin and redrawing the curves in the coordinates u_i, $(\tau_e - \tau_0)L_0/L_i$, with τ_0 = = 0.13 μsec, are shown in Fig. 3c. This graph indicates that after the stationary period is eliminated, the subsequent motion may be regarded as self-similar to the order of accuracy of the experiment.

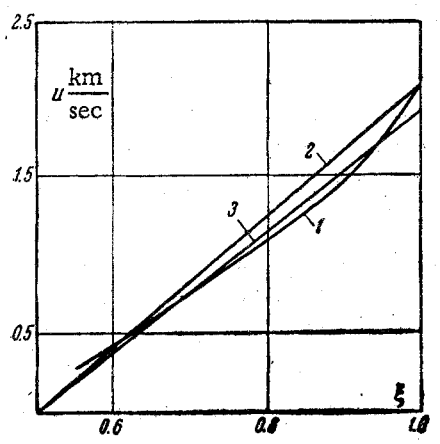

Fig. 4

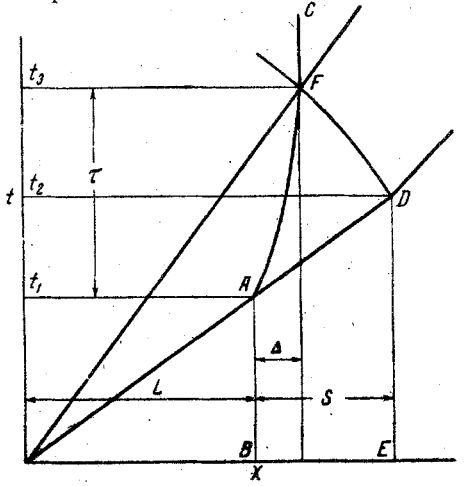

Fig. 5

Figure 4 represents the experimental results redrawn in the coordinates u, ξ (Curve 1). The transformation from the Lagrangian system, in which the experimental curves were obtained, to the Eulerian system is given by

$$\xi = \frac{x}{Dt} = \frac{1}{L_0 + D\tau}\left(L_0 + \int_0^{\tau} u(\tau)\, d\tau\right) \qquad (L_0 = 30\text{mm}). \tag{1}$$

The experimental profiles are compared in Fig. 3c and 4 with the theoretical profiles for power-law isentropes with exponents n = 3 and 2.7 (broken lines f and e in Fig. 3c, curves 3 and 2 in Fig. 4). It is clear that power-law isentropes cannot be used to described the motion of EP over distances of the order of the detonation path. Although the maximum value of mass velocity ~2.07 km/sec, which corresponds to the results of measurements by the "splitting off" method [12], corresponds to a value of the exponent n = 2.7, the whole velocity profile is better approximated in the large by the other exponent n = 3.

Recording of backward rarefaction waves. Our conclusions regarding self-similarity are confirmed by measurements of the propagation of the backward rarefaction waves.

The experimental set-up for these measurements differed from that shown in Fig. 1 only in that a paraffin block (of lower dynamic rigidity than the EP) was attached to the end face of the charge. The legs of the sensor passed through the paraffin block. In these experiments the dimensions L and S (Fig. 1 and 5) were 30 and 10-15 mm, corresponding to a measured time of ~3-5 μsec.

As a result of the interaction of the detonation wave with the interface DE (Fig. 5), the shock wave propagates into the paraffin, and a rarefaction wave DF propagates backward into the explosion products. This wave reaches the sensor at the point F. The arrival of the backward rarefaction wave changes the sign of du/dτ, which corresponds to a characteristic break in the curve u(τ). Typical oscillograms of backward rarefaction waves are shown in Fig. 6. On the second oscillogram the time scale has been also marked on the upper beam (peaks at 10 megacycle frequency).

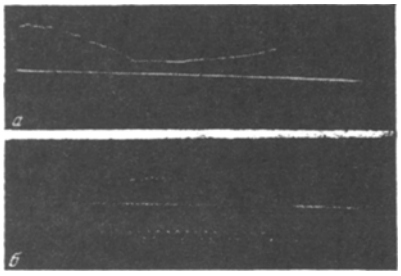

Fig. 6

The data on the propagation of the backward rarefaction waves can be used to check self-similarity, due to the fact that, as can easily be proved, in a self-similar wave the relation

$$t_2^2 = t_1 t_3 \tag{2}$$

holds (the meaning of t_i is clear from Fig. 5), which is valid for all equations of state of the EP. Relation (2) can be written in the form

$$\tau = \frac{2S}{D}\left(1 + \frac{S}{2L}\right). \tag{3}$$

From (3) it is clear that the time τ measured in the experiments depends only on the parameters L and S and on the detonation velocity, i.e., on well-known values.

The discrepancy between the experimental values of τ_e and those calculated from (3) is a measure of the deviation of the wave from self-similarity.

The experiments yielded the value $\Delta\tau = 0.14 \pm 0.04$ μsec for this difference (mean value of ten experiments with quadratic deviation). The deviation agrees in sign and magnitude with the value of τ_0 found by comparison of the curves u(τ) for charges of different lengths.

Discussion of results. Isentrope of explosion products. The deviation from self-similarity, characterized by the time τ_0, which was found in our experiments, cannot be uniquely related to the width of the stationary zone of the detonation wave. Besides the possible influence of the stationary zone, the value τ_0 may also include inaccuracies due to the small, but nevertheless finite, dimensions of the region in which the stationary regime of detonation is established, and a characteristic constant of the apparatus.

However, irrespective of the sources of the deviation from self-similarity, after the time τ_0 is subtracted from the mass velocity curves the motion can be regarded as self-similar. In this case all data on the velocity distribution can be described by a single relation u(ξ) (Fig. 4), which is obtained by averaging the four curves shown in Fig. 3c. This relation was used to calculate the isentrope of the EP.

First, note that the sharp drop of the experimental curve representing mass velocities indicates an increase in the

isentropic exponent

$$n = \left(\frac{\partial \ln p}{\partial z}\right)_S = \frac{\rho c^2}{p} \qquad (z = \ln \rho) \tag{4}$$

with decreasing density of the EP. In fact, in the case of a self-similar wave

$$\frac{du}{d\xi} = \frac{D}{1 + (\partial \ln c / \partial z)_S} \tag{5}$$

or

$$\frac{du}{d\xi} = \frac{2D}{1 + n + (\partial \ln n / \partial z)_S}, \tag{6}$$

i.e., as can be seen from (6), a large slope of $u(\xi)$, as compared with the case $n = n(\rho_j) = \text{const}$, corresponds to a negative derivative $dn/d\rho$. This proves that during the initial stages of expansion of the EP behind the detonation wavefront the isentropic exponent, determined by (4), should increase.

The fact that the slope of the curve $u(\xi)$ is not constant proves the inapplicability of Ablow's formula [9]

$$p = A\rho^n + B \qquad (A, B, n = \text{const}) \tag{7}$$

for the description of the isentrope of the EP even in a relatively narrow density range (1.5-2.3 g/cm^3). This conclusion follows directly from (5), as Eq. (7) yields $\partial \ln c/\partial z = \text{const}$.

The values of c, p, and ρ in the detonation wave, their variation behind the wavefront, and the relations between them can be easily calculated from the relation $u(\xi)$.

The speed of sound in the EP can be determined directly from the slope of the α-characteristics corresponding to the given value of the mass velocity

$$x/t = u + c\,. \tag{8}$$

This yields the relation c(u) in parametric form.

Using the well-known isentropic-flow relations $c\,d\rho = \rho\,du$ and $dp = \rho c\,du$, one can obtain by numerical integration the variation of density and pressure behind the detonation wavefront

$$\rho(\xi) = \rho_j \exp\left(\int_{u_j}^{u(\xi)} \frac{du}{c(u)}\right), \tag{9}$$

$$p(\xi) = p_j + \int_{u_j}^{u(\xi)} c(u)\,\rho(u)\,du\,. \tag{10}$$

The relations $p(\rho)$ and p(u) are obtained by eliminating the parameter ξ.

The results of calculations carried out in the above manner are given in the table.

Calculated Pressure (10^{11} bar) and Density (g/cm^3) in A Rarefaction Wave in Explosion Products

x/Dt	U/D	c/D	ρ	p
1.00	0.271	0.729	2.30	2.65
0.968	0.24	0.728	2.21	2.36
0.933	0.21	0.723	2.12	2.09
0.880	0.18	0.700	2.03	1.83
0.815	0.15	0.665	1.95	1.59
0.747	0.12	0.627	1.86	1.38
0.679	0.09	0.589	1.77	1 18
0.611	0.06	0.551	1.68	1.01
0.543	0.03	0.513	1.58	0.86
0.475	0	0.475	1.49	0.72

For illustration, Fig. 7 shows the isentrope $p(\rho)$ constructed according to the data of the table (curve 1) and, for comparison, power-law isentropes $p = A\rho^n$ for two values of the exponent n = = 2.7 and n = 3.0 (curves 2 and 3). As might be expected from a comparison of mass velocities in Fig. 3c and 4, the curve $p = A\rho^3$ lies nearer the experimental curve, although the value of the pressure and density of the EP at the Jouguet point corresponds to the other exponent n = 2.7.

The results of the calculations, as given in the table, make it possible to follow the variation of the isentropic exponent (4) during the expansion of the EP.

Figure 8 compares the relation $n(\rho)$, corresponding to the mass velocity curve in Fig. 4 (curve 1), with the data of other authors. As can be seen in Fig. 8, the relation $n(\rho)$ obtained here practically coincides in the region of densities near the Jouguet density with the curve calculated for Composition "B" (TH 35/65) according to Ablow's formula [9] (curve 2), where the constants have been determined from the attenuation of shock waves in obstacles. For EP densities below

2 g/cm^3 Ablow's equation is not valid.

Figure 8 also shows the relation n(ρ) for the same Composition "B" corresponding to the Kistiakowsky-Wilson equation of state [13] (curve 3). Comparing this relation with the experimental curves, one clearly sees that the Kistiakowsky-Wilson equation of state should lead to velocity distributions markedly different from the experimental curve shown in Fig. 4. It is also clear that calculations based on this equation of state should lead to slower attenuation of shock waves in obstacles than that observed experimentally.

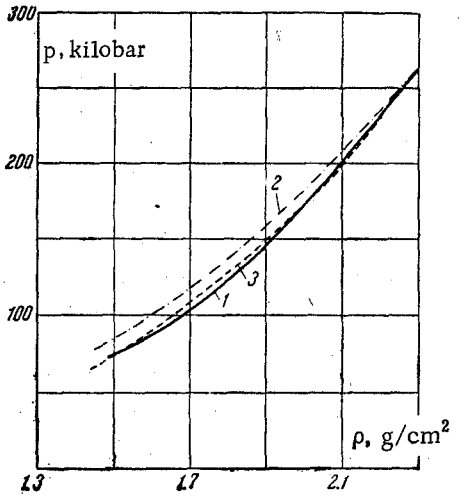

Fig. 7

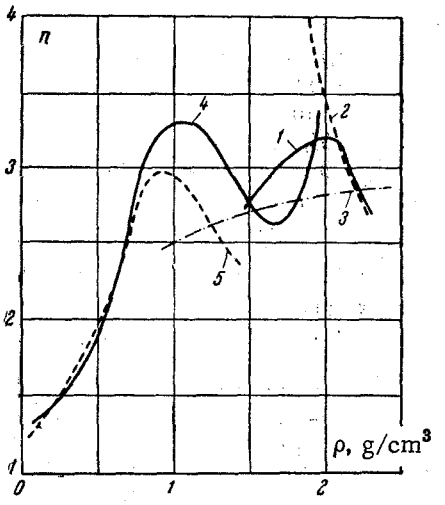

Fig. 8

Relations 4 and 5 of Fig. 8, calculated by Jones and Miller [3] for TNT with two initial densities (1.5 and 1.0 g/cm^3), are more complicated in form. The maxima of these curves are strongly shifted toward low densities. The difference between the compositions of the EP of TNT and TH 50/50 makes it impossible to draw definite conclusions from the comparison, but such large a displacement of the maximum of n(ρ) for TNT seems improbable.

REFERENCES

1. Ya. B. Zel'dovich, "On the distribution of pressure and velocity in detonation products, in particular in the case of spherical wave propagation," Zh. eksper. i teor. fiz., vol. 12, p. 389, 1942.

2. G. I. Taylor, "The dynamics of the combustion products behind plane and spherical detonation fronts in explosives," Proc. Roy. Soc. A, vol. 200, p. 235, 1950.

3. H. Jones and A. R. Miller, "The detonation of solid explosives," Proc. Roy. Soc. A, vol. 194, p. 480, 1948.

4. R. W. Goranson et al., "Dynamic determination of the compressibility of metals," J. Appl. Phys., vol. 26, p. 1472, 1955.

5. L. V. Al'tshuler, K. K. Krupnikov, B. N. Ledenev, V. I. Zhuchikhin, and M. I. Brazhnik, "Dynamic compressibility and equation of state of iron at high pressures," Zh. Eksper. i teor. fiz., vol. 34, p. 874, 1958.

6. W. E. Deal, "The measurements of c – j pressure for explosive," J. Chem. Phys., vol. 27, p. 796, 1957.

7. R. E. Duff and E. Houston, "Measurements of the c – j pressure and reaction zone length in a detonating high explosive," J. Chem. Phys., vol. 23, p. 1268, 1955.

8. A. N. Dremin and P. F. Pokhil, "Parameters of the detonation waves of TNT, hexogen, nitroglycerine, and nitromethane," DAN SSSR, vol. 128, p. 989, 1959.

9. W. E. Drummond, "Explosive induced shock waves," J. Appl. Phys., vol. 28, p. 1437, 1957.

10. V. M. Zaitsev, P. F. Pokhil, and K. K. Shvedov, "Electromagnetic method of measuring the velocity of explosion products," DAN SSSR, vol. 132, p. 1339, 1960.

11. A. A. Brish, M. S. Tarasov, and V. A. Tsukerman, "Electrical conductivity of the explosion products of solid explosives," Zh. eksper. i teor. fiz., vol. 37, p. 1543, 1959.

12. A. N. Dremin and G. A. Adadurov, "Parameters of detonation of TNT-hexane mixtures," Izv. AN SSSR, Otd. khim. n., 6, 1130, 1960.

13. R. O. Cowan and W. Fickett, "Calculation of the detonation properties of solid explosives with the Kistiakowsky-Wilson equation of state," J. Chem. Phys., vol. 24, p. 932, 1956.

18 September 1964 Moscow